Inorganic Chemistry
Article

*Inorg. Chem.* **2009**, *48*, 7059–7065 **7059**
DOI: 10.1021/ic802443n

# A Series of New Infrared NLO Semiconductors, $ZnY_6Si_2S_{14}$, $Al_xDy_3(Si_yAl_{1-y})S_7$, and $Al_{0.33}Sm_3SiS_7$

**Sheng-Ping Guo,[†,‡] Guo-Cong Guo,*[,†] Ming-Sheng Wang,[†] Jian-Ping Zou,[†] Gang Xu,[†] Guo-Jian Wang,[†] Xi-Fa Long,[†] and Jin-Shun Huang[†]**

[†]*State Key Laboratory of Structural Chemistry, Fujian Institute of Research on the Structure of Matter, Chinese Academy of Sciences, Fuzhou 350002, P. R. China, and* [‡]*Graduate School of Chinese Academy of Sciences, Beijing 100039, P. R. China*

Received October 23, 2008

Four new quaternary isostructural rare-earth thiosilicates, $ZnY_6Si_2S_{14}$ (**1**), $Al_{0.50}Dy_3(Si_{0.50}Al_{0.50})S_7$ (**2**), $Al_{0.38}Dy_3(Si_{0.85}Al_{0.15})S_7$ (**3**), and $Al_{0.33}Sm_3SiS_7$ (**4**), crystallized in the chiral and polar space group $P6_3$, have been prepared by a facile synthetic routine. Compounds **1**−**3** show strong second harmonic generation effects at 2.1 um with the intensities of **1**, **2**, and **3** being about 2, 2, and 1 times that of KTP ($KTiOPO_4$), respectively. The calculated band structure of **1** implies that the optical absorptions of $BLn_6M_2Q_{14}$ and $ALn_3MQ_7$ family compounds are mainly ascribed to the charge transitions from Q−p to Ln−4f (4d for Y) states. Compounds **2**−**4** exhibit antiferromagnetic-like interactions.

## Introduction

Many efforts in solid-state chemistry have been made to engineer new inorganic compounds with desired physical properties. In particular, crystallographically noncentrosymmetric (NCS) compounds have received much attention due to their special properties, such as piezoelectricity, pyroelectricity, ferroelectricity, and second-order nonlinear optical (NLO) activity.[1] These properties give the NCS compounds potential applications in some special regions.[2] As a NCS structure is the prerequisite for these properties, the controllable syntheses of NCS compounds are challenging. To date, some synthetic strategies for NCS inorganic compounds are employed, as follows: (1) the incorporation of $d^0$ transition-metal cations such as $Ti^{4+}$, $Zr^{4+}$, $Hf^{4+}$, $V^{5+}$, $Nb^{5+}$, $Ta^{5+}$, $Mo^{6+}$, and $W^{6+}$ and main group cations with nonbonded electron pairs such as $Pb^{2+}$, $Sb^{3+}$, $Bi^{3+}$, $Se^{4+}$, $Te^{4+}$, and $I^{5+}$, both of which are susceptible to second-order Jahn−Teller distortions;[1,3,4] (2) the use of chiral organic molecules or metal complexes as templating agents;[5] (3) salt inclusion;[6]

*To whom correspondence should be addressed. Phone: +86 591 83705882. Fax: +86 591 83714946. E-mail: gcguo@fjirsm.ac.cn.

(1) (a) Ok, K. M.; Chi, E. O.; Halasyamani, P. S. *Chem. Soc. Rev.* **2006**, *35*, 710. (b) Muller, E. A.; Cannon, R. J.; Sarjeant, A. N.; Ok, K. M.; Halasyamani, P. S.; Norquist, A. J. *Cryst. Growth Des.* **2005**, *5*, 1913.

(2) (a) Scott, J. F. *Science* **2007**, *315*, 954. (b) Chen, C. T.; Liu, G. Z. *Annul. Rev. Mater. Sci.* **1986**, *16*, 203. (c) Eaton, D. F. *Science* **1991**, *253*, 281. (d) Kim, Y.; Martin, S. W.; Ok, K. M.; Halasyamani, P. S. *Chem. Mater.* **2005**, *17*, 2046.

(3) (a) Halasyamani, P. S.; Poeppelmeier, K. R. *Chem. Mater.* **1998**, *10*, 2753. (b) Jiang, H. L.; Huang, S. P.; Fan, Y.; Mao, J. G.; Cheng, W. D. *Chem.—Eur. J.* **2008**, *14*, 1972. (c) Sivakumar, T.; Chang, H. Y.; Back, J.; Halasyamani, P. S. *Chem. Mater.* **2007**, *19*, 4710. (d) Goodey, J.; Broussard, J.; Halasyamani, P. S. *Chem. Mater.* **2002**, *14*, 3174. (e) Kim, J. H.; Back, J.; Halasyamani, P. S. *Chem. Mater.* **2007**, *19*, 5637. (f) Porter, Y.; Ok, K. M.; Bhuvanesh, N. S. P.; Halasyamani, P. S. *Chem. Mater.* **2001**, *13*, 1910. (g) Ok, K. M.; Halasyamani, P. S. *Angew. Chem., Int. Ed.* **2004**, *43*, 5489. (h) Marvel, M. R.; Lesage, J.; Baek, J.; Halasyamani, P. S.; Stern, C. L.; Poeppelmeier, K. R. *J. Am. Chem. Soc.* **2007**, *129*, 13963. (i) Jiang, H. L.; Kong, F.; Fan, Y.; Mao, J. G. *Inorg. Chem.* **2008**, *47*, 7430. (j) Phanon, D.; Gautier-Luneau, I. *Angew. Chem., Int. Ed.* **2007**, *46*, 8488. (k) Halasyamani, P. S. *Chem. Mater.* **2004**, *16*, 3586. (l) Ok, K. M.; Halasyamani, P. S. *Chem. Mater.* **2006**, *18*, 3176. (m) Halasyamani, P. S.; Poeppelmeier, K. R. *Inorg. Chem.* **2008**, *47*, 8427. (n) Hubbard, D. J.; Johnston, A. R.; Casalongue, H. S.; Sarjeant, A. N.; Norquist, A. L. *Inorg. Chem.* **2008**, *47*, 8518. (o) Kim, J. H.; Halasyamani, P. S. *J. Solid State Chem.* **2008**, *181*, 2108. (p) Kong, F.; Huang, S. P.; Sun, Z. M.; Mao, J. G.; Cheng, W. D. *J. Am. Chem. Soc.* **2006**, *128*, 7750. (q) Ra, H. S.; Ok, K. M.; Halasyamani, P. S. *J. Am. Chem. Soc.* **2003**, *125*, 7764. (r) Chang, H. Y.; Sivakumar, T.; Ok, K. M.; Halasyamani, P. S. *Inorg. Chem.* **2008**, *47*, 8511. (s) Zhang, W. G.; Tao, X. T.; Zhang, C. Q.; Gao, Z. L.; Zhang, Y. Z.; Yu, W. T.; Cheng, X. F.; Liu, X. S.; Jiang, M. H. *Cryst. Growth Des.* **2008**, *8*, 304. (t) Chi, E. O.; Gandini, A.; Ok, K. M.; Zhang, L.; Halasyamani, P. S. *Chem. Mater.* **2004**, *16*, 3616.

(4) (a) Ok, K. M.; Bhuvanesh, N. S. P.; Halasyamani, P. S. *Inorg. Chem.* **2001**, *40*, 1978. (b) Ok, K. M.; Bhuvanesh, N. S. P.; Halasyamani, P. S. *J. Solid State Chem.* **2001**, *161*, 57. (c) Sykora, R. E.; Ok, K. M.; Halasyamani, P. S.; Wells, D. M.; Albrecht-Schmitt, T. E. *Inorg. Chem.* **2002**, *14*, 2741. (d) Shehee, T. C.; Sykora, R. E.; Kang, M. K.; Halasyamani, P. S.; Albrecht-Schmitt, T. E. *Inorg. Chem.* **2003**, *42*, 457. (e) Sykora, R. E.; Ok, K. M.; Halasyamani, P. S.; Albrecht-Schmitt, T. E. *J. Am. Chem. Soc.* **2002**, *124*, 1951. (f) Porter, Y.; Bhuvanesh, N. S. P.; Halasyamani, P. S. *Inorg. Chem.* **2001**, *40*, 1172. (g) Goodey, J.; Ok, K. M.; Broussard, J.; Hofmann, C.; Escobedo, F. V.; Halasyamani, P. S. *J. Solid State Chem.* **2003**, *175*, 3. (h) Wickleder, M. S.; Buchner, O.; Wickleder, C.; Sheik, S.; Brunklaus, G.; Eckert, H. *Inorg. Chem.* **2004**, *43*, 5860. (i) Chi, E. O.; Ok, K. M.; Porter, Y.; Halasyamani, P. S. *Chem. Mater.* **2006**, *18*, 2070. (j) Pan, S. L.; Smit, J. P.; Marvel, M. R.; Stampler, E. S.; Haag, J. M.; Baek, J.; Halasyamani, P. S.; Poeppelmeier, K. P. *J. Solid State Chem.* **2008**, *181*, 2087. (k) Henderson, N. L.; Baek, J.; Halasyamani, P. S.; Schaak, R. E. *Chem. Mater.* **2007**, *19*, 1883.

(5) (a) Che, S.; Liu, Z.; Ohsuna, T.; Sakamoto, K.; Terasaki, O.; Tatsumi, T. *Nature* **2004**, *429*, 281. (b) Lin, C. H.; Wang, S. L. *Chem. Mater.* **2002**, *14*, 96. (c) Bu, X.; Zheng, N.; Li, Y.; Feng, P. *J. Am. Chem. Soc.* **2003**, *125*, 6024.

(6) (a) Queen, W. L.; West, J. P.; Hwu, S.-J.; Derveer, D. G.; Zarzyczny, M. C.; Pavlick, R. A. *Angew. Chem., Int. Ed.* **2008**, *47*, 3791. (b) Huang, Q.; Hwu, S. J. *Inorg. Chem.* **2003**, *42*, 655. (c) Mo, X. H.; Ferguson, E.; Hwu, S. J. *Inorg. Chem.* **2005**, *44*, 3121. (d) Li, R. K.; Yu, Y. *Inorg. Chem.* **2006**, *45*, 6840. (e) Choudhury, A.; Polyakova, L. A.; Strobel, S.; Dorhout, P. K. *J. Solid State Chem.* **2007**, *180*, 1381. (f) Mo, X. H.; Hwu, S. J. *Inorg. Chem.* **2003**, *42*, 3978.


Published on Web 07/09/2009

(4) acentric packing of helical chains via directed ligands;[7] (5) introduction of acentric tetrahedral blocks;[8] and (6) the combination of two or more kinds of coordination centers with different sizes, coordination numbers, and packing characteristics.[9] These strategies make it possible that a compound will crystallize with a NCS space group greater than a centrosymmetric one.

There has been much interest in NLO crystals shown by many chemists and crystallographers. A number of practicable ultraviolet (UV) NLO crystals have been synthesized;[10] however, practicable infrared (IR) NLO crystals are still relatively rare.[11] NCS chalcogenides may surpass the well-established oxide counterparts in their NLO properties in the IR region, as they have wider mid- and far-IR transmission windows.[9,11] In particular, a variety of chalcogenides generally formulated as $BLn_6M_2Q_{14}$ or $ALn_3MQ_7$ (A = alkali or coinage metal; B = divalent metal; M = Si, Ge, Sn; Q = S, Se) crystallize in the chiral space group $P6_3$, and they were thought to be potential IR NLO compounds,[12] of which only $CuLa_3GeSe_7$ was reported to exhibit weak second harmonic generation (SHG) signals. On the other hand, the ferroelectric properties of the $BLn_6M_2Q_{14}$ and $ALn_3MQ_7$ family compounds were predicted in 1990;[13] however, to the best of our knowledge, no $BLn_6M_2Q_{14}$ or $ALn_3MQ_7$ compounds have been reported with ferroelectric properties.

Our recent efforts in synthesizing NCS chalcogenides have focused largely on the system of M′−Ln−M−Q (M′ = main group or transition metal), combining the above numbers 5 and 6 synthetic strategies.[14] Herein, we demonstrate a facile synthetic method to obtain four new quaternary chalcogenides, $ZnY_6Si_2S_{14}$ (**1**), $Al_{0.50}Dy_3(Si_{0.50}Al_{0.50})S_7$ (**2**), $Al_{0.38}Dy_3(Si_{0.85}Al_{0.15})S_7$ (**3**), and $Al_{0.33}Sm_3SiS_7$ (**4**), and their crystal and electronic structures and magnetic and NLO properties are also reported. Remarkably, compounds **1**−**3** show stronger SHG intensities among the $BLn_6M_2Q_{14}$ and $ALn_3MQ_7$ family compounds.

## Experimental Section

**Reagents and Syntheses.** All starting materials were used as received without further purification. Single crystals of the four compounds were obtained by solid-state reactions with KI as a flux. Compound **1** was crystallized from the reaction containing ZnS (70 mg, 0.718 mmol, 99%), Si (40 mg, 1.424 mmol, 99%), S (183 mg, 5.708 mmol, 99.999%), $Y_2O_3$ (161 mg, 0.713 mmol, 99.9%), B (46 mg, 4.255 mmol, 99%), and KI (400 mg, 2.410 mmol, 99%). Compounds **2** and **3** were crystallized from separate reactions containing Al (6 mg, 0.222 mmol, 99%), Si (37 mg, 1.317 mmol, 99%), S (169 mg, 5.271 mmol, 99.999%), $Dy_2O_3$ (246 mg, 0.660 mmol, 99.9%), B (43 mg, 3.978 mmol, 99%), and KI (400 mg, 2.410 mmol, 99%). Compound **4** was crystallized from the reaction containing Al (6 mg, 0.222 mmol, 99%), Si (38 mg, 1.353 mmol, 99%), S (174 mg, 5.427 mmol, 99.999%), $Sm_2O_3$ (237 mg, 0.680 mmol, 99.9%), B (44 mg, 4.070 mmol, 99%), and KI (400 mg, 2.410 mmol, 99%). All of the mixtures of starting materials were ground into fine powders in an agate mortar and pressed into pellets, followed by being loaded into quartz tubes. The tubes were evacuated at $1 \times 10^{-4}$ Torr and flame-sealed. The samples were placed into a furnace, heated from room temperature to 300 °C over 5 h, kept at 300 °C for 10 h, heated to 650 °C over 5 h, kept at 650 °C for 10 h, heated to 950 °C over 5 h, kept at 950 °C for 10 days, then cooled down to 300 °C over 5 days, and powered off. Yellow block crystals of **1**−**4** were hand-picked under a microscope, and their purities were confirmed in an X-ray diffraction (XRD) study. They are stable in the presence of air and water and show no signs of appreciable change in crystal quality over several months. The yield of compound **4** is 76% based on Sm, and the others are less than 10% based on Ln.

**Structure Determination.** For **1**, a single crystal with dimensions of $0.20 \times 0.12 \times 0.06$ mm$^3$ was mounted on a glass fiber for single-crystal X-ray diffraction analysis. The measurement was performed on a Rigaku Scxmini CCD diffractometer equipped with graphite-monochromated Mo Kα radiation ($\lambda = 0.71073$ Å) at 293 K. The intensity data set was collected with an $\omega$ scan technique and reduced using the CrystalClear software.[15]

For **2**−**4**, the respective single crystals were mounted on a glass fiber for single-crystal X-ray diffraction analysis. All of the measurements were performed on a Rigaku AFC7R diffractometer equipped with graphite-monochromated Mo Kα radiation ($\lambda = 0.71073$ Å) at 293 K. Intensity data sets were collected with an $\omega$-$2\theta$ scan technique and reduced using the CrystalStructure software.[16]

The structures of **1**−**4** were solved by direct methods and refined by full-matrix least-squares techniques on $F^2$ with anisotropic thermal parameters for all atoms. All of the calculations were performed with the Siemens SHELXTL version 5 package of crystallographic software.[17] The formulas are based on taking

(7) (a) Maggard, P. A.; Stern, C. L.; Poeppelmeier, K. R. *J. Am. Chem. Soc.* **2001**, *123*, 7742. (b) Fu, M. L.; Guo, G. C.; Liu, X.; Zou, J. P.; Huang, J. S. *Cryst. Growth Des.* **2007**, *7*, 2387.

(8) (a) Kim, Y.; Seo, I.-S.; Martin, S. W.; Baek, J.; Halasyamani, P. S.; Arumugam, N.; Steinfink, H. *Chem. Mater.* **2008**, *20*, 6048. (b) Huang, F. Q.; Choe, W.; Lee, S.; Chu, J. S. *Chem. Mater.* **1998**, *10*, 1320. (c) Gitzendanner, R. L.; DiSalvo, F. J. *Inorg. Chem.* **1996**, *35*, 2623. (d) Sambrook, T.; Smura, C. F.; Clarke, S. J.; Ok, K. M.; Halasyamani, P. S. *Inorg. Chem.* **2007**, *46*, 2571.

(9) Liao, J. H.; Marking, G. M.; Hsu, K. F.; Matsushita, Y.; Ewbank, M. D.; Borwick, R.; Cunningham, P.; Rosker, M. J.; Kanatzidis, M. G. *J. Am. Chem. Soc.* **2003**, *125*, 9484.

(10) (a) Chen, C.; Lin, C.; Wang, Z. *Appl. Phys. B: Laser Opt.* **2005**, *80*, 1. (b) Chen, C. T.; Wang, Y. B.; Wu, B. C.; Wu, K. C.; Zeng, W. L.; Yu, L. H. *Nature* **1995**, *373*, 322. (c) Becker, P. *Adv. Mater.* **1998**, *10*, 979 and references therein. (d) Chen, C. T.; Bai, L.; Wang, Z. Z.; Li, R. K. *J. Cryst. Growth* **2006**, *292*, 169 and references therein.

(11) (a) Ohmer, M. C.; Goldstein, J. T.; Zelmon, D. E.; Saxler, A. W.; Hegde, S. M.; Wolf, J. D.; Schunemann, P. G.; Pollak, T. M. *J. Appl. Phys.* **1999**, *86*, 94. (b) Isaenko, L.; Krinitsin, P.; Vedenyapin, V.; Yelisseyev, A.; Merkulov, A.; Zondy, J. J.; Petrov, V. *Cryst. Growth Des.* **2005**, *5*, 1325. (c) Isaenko, L.; Yelisseyev, A.; Lobanov, S. *J. Appl. Phys.* **2002**, *91*, 9475. (d) Feigelson, R. S. *J. Cryst. Growth* **2006**, *292*, 179. (e) Li, G. H.; Su, G. B.; Zhuang, X. X.; Li, Z. D.; He, Y. P. *Opt. Mater.* **2004**, *27*, 539.

(12) (a) Huang, F. Q.; Ibers, J. A. *Acta Crystallogr.* **1999**, *C55*, 1210. (b) Wu, L. B.; Huang, F. Q. *Z. Kristallogr. NCS* **2005**, *220*, 307. (c) Yang, Y. T.; Ibers, J. A. *J. Solid State Chem.* **2000**, *155*, 433. (d) Hartenbach, I.; Müller, A. C.; Schleid, T. *Z. Anorg. Allg. Chem.* **2006**, *632*, 2147. (e) Hwu, S. J.; Bucher; Carpenter, J. D.; Taylor, S. P. *Inorg. Chem.* **1995**, *34*, 1979. (f) Huch, M. R.; Gulay, L. D.; Olekseyuk, I. D. *J. Alloys Compd.* **2006**, *424*, 114. (g) Jin, Z. S.; Li, Z. T.; Du, Y. R. *Yingyong Huaxue* **1985**, *2*, 42. (h) Hartenbach, I.; Nilges, T.; Schleid, T. *Z. Anorg. Allg. Chem.* **2007**, *633*, 2445. (i) Collin, G.; Laruelle, P. *C. R. Hebdomadaires Seances Acad. Sci., Ser. C* **1970**, *270*, 410. (j) Collin, G.; Etienne, J.; Laruelle, P. *Bull. Soc. Fr. Mineral. Cristallogr.* **1973**, *96*, 12. (k) Hartenbach, I.; Schleid, T. *J. Solid State Chem.* **2003**, *171*, 382. (l) Perez, G.; Darriet, M. *C. R. Hebdomadaires Seances Acad. Sci., Ser. C* **1970**, *270*, 420. (m) Gitzendanner, R. L.; Spencer, C. M.; DiSalvo, F. J.; Pell, M. A.; Ibers, J. A. *J. Solid State Chem.* **1996**, *131*, 399. (n) Gulay, L. D.; Kaczorowski, D.; Pietraszko, A. *J. Alloys Compd.* **2005**, *403*, 49.

(13) Abrahams, S. C. *Acta Crystsllogr., Sect. B* **1990**, *46*, 311.

(14) (a) Zeng, H. Y.; Zheng, F. K.; Guo, G. C.; Huang, J. S. *J. Alloys Compd.* **2007**, DOI: 10.1016/j.jallcom.2007.03.136. (b) Zeng, H. Y. Ph.D. Dissertation, Fujian Institute of Research on the Structure of Matter, Chinese Academy of Sciences, **1998**. (c) Lin, S. H.; Mao, J. G.; Guo, G. C.; Huang, J. S. *J. Alloys Compd.* **1997**, *252*, L8.

(15) Rigaku, *CrystalClear*, version 1.3.5; Rigaku Corporation: Tokyo, 2002.

(16) Rigaku, *CrystalStructure Version 3.6.0*, Rigaku Corporation: Tokyo, 2002.

(17) Siemens, *SHELXTL Version 5 Reference Manual*; Siemens Energy & Automation Inc.: Madison, WI, 1994.

**Table 1.** Crystal Data and Structure Refinement Parameters

| | $ZnY_6Si_2S_{14}$ | $Al_{0.50}Dy_3(Si_{0.50}Al_{0.50})S_7$ | $Al_{0.38}Dy_3(Si_{0.85}Al_{0.15})S_7$ | $Al_{0.33}Sm_3SiS_7$ |
|---|---|---|---|---|
| chemical formula | (**1**) | (**2**) | (**3**) | (**4**) |
| fw | 1103.85 | 752.98 | 750.27 | 712.46 |
| cryst size ($mm^3$) | 0.20 × 0.12 × 0.06 | 0.16 × 0.06 × 0.02 | 0.08 × 0.06 × 0.04 | 0.10 × 0.10 × 0.10 |
| $T$ (K) | 293(2) | 293(2) | 293(2) | 293(2) |
| $\lambda$ (Mo Kα, Å) | 0.71073 | 0.71073 | 0.71073 | 0.71073 |
| cryst syst | hexagonal | hexagonal | hexagonal | hexagonal |
| space group | $P6_3$ (173) | $P6_3$ (173) | $P6_3$ (173) | $P6_3$ (173) |
| $a$ (Å) | 9.807(1) | 9.636(1) | 9.776(1) | 9.979(1) |
| $c$ (Å) | 5.640(1) | 5.944(1) | 5.682(1) | 5.679(1) |
| $V$ ($Å^3$) | 469.8(1) | 478.0(1) | 470.2(1) | 489.8(1) |
| $Z$ | 1 | 2 | 2 | 2 |
| $D_{calcd}$ (g $cm^{-3}$) | 3.902 | 5.232 | 5.298 | 4.831 |
| $\mu$ ($mm^{-1}$) | 21.229 | 24.816 | 25.225 | 19.318 |
| $F$(000) | 516 | 660 | 658 | 633 |
| $\theta$ range (deg) | 4.34−25.48 | 4.21−25.32 | 2.41−25.46 | 2.36−25.46 |
| measd. reflns | 3075 | 415 | 1046 | 409 |
| indep. reflns/$R_{int}$ | 586/0.0469 | 329/0.0376 | 325/0.0458 | 334/0.0215 |
| obsd reflns | 584 | 321 | 316 | 308 |
| R1[a] ($I > 2\sigma(I)$) | 0.0209 | 0.0226 | 0.0226 | 0.0255 |
| wR2[b] (all data) | 0.0481 | 0.0592 | 0.0581 | 0.0508 |
| GOF on $F^2$ | 1.002 | 1.000 | 1.011 | 1.052 |
| $\Delta\rho_{max}/\Delta\rho_{min}$, e/$Å^3$ | 0.480/−0.487 | 1.088/−1.047 | 0.947/−1.430 | 1.030/−0.962 |

[a] $R1 = ||F_o| - |F_c||/|F_o|$. [b] $wR2 = [w(F_o^2 - F_c^2)^2]/[w(F_o^2)^2]^{1/2}$.

collectively into account crystallographically refined compositions and requirements of charge neutrality, and disorders were found in the A or B or the M sites of the four compounds.

The crystallographic data are listed in Table 1. Selected bond lengths are given in Table 2. The atomic coordinates and thermal parameters are listed in Table S1 (Supporting Information). Further details of the crystal structure investigations can be obtained from the Fachinformationszentrum Karlsruhe, 76344 Eggenstein-Leopoldshafen, Germany (fax: (49) 7247−808−666; e-mail: crysdata@fiz-karlsruhe.de) on quoting the depository numbers CSD-419991 for **1**, CSD-419992 for **2**, CSD-419993 for **3**, and CSD-419990 for **4**.

**Powder XRD.** The powder XRD patterns were collected with a Rigaku DMAX 2500 diffractometer at 40 kV and 100 mA or a PANalytical X'Pert Pro diffractometer at 40 kV and 40 mA for Cu Kα radiation ($\lambda$ = 1.5406 Å) with a scan speed of 5°/min at room temperature. The simulated patterns were produced using the Mercury program and single-crystal reflection data. Figure S1 (Supporting Information) gives the powder XRD patterns of the four compounds, which correspond well with the simulated ones, confirming the high purities of the prepared samples.

**Infrared and UV−Vis−NIR Diffuse Reflectance Spectroscopies.** The diffuse reflectance spectra were recorded at room temperature on a computer-controlled Lambda 900 UV−Vis−NIR spectrometer equipped with an integrating sphere in the wavelength range of 300−1700 nm. A $BaSO_4$ plate was used as a reference, on which the finely ground powders of the samples were coated. The absorption spectra were calculated from reflection spectra using the Kubelka−Munk function.[18] The IR spectra were recorded by using a Nicolet Magana 750 FT-IR spectrophotometer in the range of 4000−400 $cm^{-1}$. Powdery samples were pressed into pellets with KBr. No FT-IR absorption peaks of **1**−**4** are in the range 4000−700 $cm^{-1}$.

**SHG Measurements.** Powder SHG measurements on hand-selected crystalline samples were performed on a modified Kurtz-NLO system using 1.06 and 2.1 $\mu$m laser radiation. The output signals were detected by a photomultiplier, and KTP ($KTiOPO_4$) powder sieved with 70 meshes (∼150 um) was used as a comparison. Compound **4** was sieved to the same size with KTP, while compounds **1**−**3** were incapable of being sieved in view of their low yields. The SHG effects of compounds **1**−**4** with a particle size of ∼20 um (Figure S8, Supporting Information) and compound **4** sieved with 70 meshes (∼150 um) were measured with the graded powdery KTP as a reference.

**Ferroelectricity Measurement.** The ferroelectricity of **4** was measured using a virtual ground mode. The graph was obtained by analyzing a pellet (silver paste was applied to both sides) of the powdery sample on a TF2000 ferroelectric tester while the sample was immerged in insulating oil.

**Magnetic Properties.** The variable-temperature magnetic susceptibilities were measured with a Quantum Design PPMS model 6000 magnetometer in the temperature range 2−300 K at a field of 5000 Oe, and diamagnetic corrections were made using Pascal's constants.

**Computational Procedures.** The crystallographic data of **1** determined by single-crystal X-ray diffraction analysis were used to calculate its electronic band structure. The calculation of the electronic band structure along with the densities of state (DOS) was performed with the CASTEP code on the basis of density functional theory using a plane-wave expansion of the wave functions and a norm-conserving pseudopotential,[19] in which the orbital electrons of Y−$4d^1 5s^2$, S−$3s^2 3p^4$, Si−$3s^2 3p^2$, and Zn−$3d^{10} 4s^2$ were treated as valence electrons. The number of plane waves included in the basis was determined using a cutoff energy of 400 eV, and the numerical integration of the Brillouin zone was performed using a 1×1×1 Monkhorst−Pack $k$-point sampling.

## Results and Discussion

Generally, reactive-flux alkali-metal (poly)chalcogenides, which are air-sensitive, were commonly used in the syntheses of metal chalcogenides in a glovebox.[20] In our experiments,

(18) (a) Wendlandt, W. W.; Hecht, H. G. *Reflectance Spectroscopy*; Interscience Publishers: New York, 1966. (b) Kortüm, G. *Reflectance Spectroscopy*; Springer: New York, 1969.

(19) (a) Hamann, D. R.; Schluter, M.; Chiang, C. *Phys. Rev. Lett.* **1979**, *43*, 1494. (b) Segall, M.; Linda, P.; Probert, M.; Pickard, C.; Hasnip, P.; Clark, S.; Payne, M. *J. Phys.: Condens. Matter* **2002**, *14*, 2717. (c) Perdew, J. P.; Burke, K.; Ernzerhof, M. *Phys. Rev. Lett.* **1996**, *77*, 3865. (d) Zou, J. P.; Wu, D. S.; Huang, S. P.; Zhu, J.; Guo, G. C.; Huang, J. S. *J. Solid State Chem.* **2007**, *180*, 805.

(20) (a) Sunshine, S. A.; Kang, D.; Ibers, J. A. *J. Am. Chem. Soc.* **1987**, *109*, 6202. (b) Kanatzidis, M. G. *Chem. Mater.* **1990**, *2*, 353. (c) Sutorik, A. C.; Kanatzidis, M. G. *Chem. Mater.* **1997**, *9*, 387. (d) Kanatzidis, M. G.; Sutorik, A. C. *Prog. Inorg. Chem.* **1995**, *43*, 151.

**Table 2.** Selected Bond Distances (Å)[a]

**1**

| bond | dist. | bond | dist. | bond | dist. |
|---|---|---|---|---|---|
| Y(1)−S(2)#1 | 2.728(1) | Y(1)−S(3)#4 | 2.871(1) | Zn(1)−S(2) | 2.537(2) |
| Y(1)−S(2) | 2.748(1) | Y(1)−S(1) | 2.933(1) | Zn(1)−S(2)#6 | 2.617(2) |
| Y(1)−S(3)#2 | 2.776(1) | Y(1)−S(3)#5 | 2.957(1) | Si(1)−S(1) | 2.088(3) |
| Y(1)−S(2)#3 | 2.818(2) | Y(1)−S(2)#6 | 3.115(2) | Si(1)−S(3) | 2.133(1) |

**2**

| bond | dist. | bond | dist. | bond | dist. |
|---|---|---|---|---|---|
| Dy(1)−S(2)#1 | 2.724(1) | Dy(1)−S(1) | 2.808(1) | Al(1)−S(2) | 2.504(4) |
| Dy(1)−S(3)#2 | 2.767(1) | Dy(1)−S(3)#4 | 2.850(2) | Al(1)−S(2)#1 | 2.507(4) |
| Dy(1)−S(2)#3 | 2.786(1) | Dy(1)−S(3)#5 | 2.997(1) | Si(1)−S(1) | 2.166(4) |
| Dy(1)−S(2) | 2.804(2) | Dy(1)−S(2)#8 | 3.530(1) | Si(1)−S(3) | 2.195(2) |

**3**

| bond | dist. | bond | dist. | bond | dist. |
|---|---|---|---|---|---|
| Dy(1)−S(2)#1 | 2.716(1) | Dy(1)−S(3)#4 | 2.872(1) | Al(1)−S(2)#1 | 2.549(2) |
| Dy(1)−S(2)#2 | 2.739(1) | Dy(1)−S(1) | 2.918(1) | Al(1)−S(2)#7 | 2.551(2) |
| Dy(1)−S(3)#3 | 2.782(1) | Dy(1)−S(3)#5 | 2.967(1) | Si(1)−S(1) | 2.098(2) |
| Dy(1)−S(2) | 2.809(1) | Dy(1)−S(2)#3 | 3.184(1) | Si(1)−S(3) | 2.135(1) |

**4**

| bond | dist. | bond | dist. | bond | dist. |
|---|---|---|---|---|---|
| Sm(1)−S(2)#1 | 2.771(1) | Sm(1)−S(3)#5 | 2.991(1) | Al(1)−S(2) | 2.569(6) |
| Sm(1)−S(2) | 2.778(1) | Sm(1)−S(2)#6 | 3.124(2) | Al(1)−S(2)#6 | 2.585(6) |
| Sm(1)−S(3)#2 | 2.829(1) | Sm(1)−S(3)#4 | 2.927(1) | Si(1)−S(1) | 2.087(3) |
| Sm(1)−S(2)#3 | 2.883(2) | Sm(1)−S(1) | 2.985(1) | Si(1)−S(3) | 2.136(2) |

[a] Symmetry codes. Compound **1**: (#1) $-x+y, -x, z$; (#2) $x, y, z-1$; (#3) $y, -x+y, z+1/2$; (#4) $-x+y, -x+1, z-1$; (#5) $-x+1, -y+1, z-1/2$; (#6) $y, -x+y, z-1/2$. Compound **2**: (#1) $x-y+1, x+1, z-1/2$; (#2) $x, y, z-1$; (#3) $y-1, -x+y, z-1/2$; (#4) $-y+1, x-y+1, z-1$; (#5) $-x+1, -y+2, z-1/2$; (#6) $-y+1, x-y+2, z$; (#7) $-x+y-1, -x+1, z$; (#8) $-x, -y+2, z-1/2$. Compound **3**: (#1) $x-y+1, x+1, z-1/2$; (#2) $y-1, -x+y, z-1/2$; (#3) $x, y, z-1$; (#4) $-y+1, x-y+1, z-1$; (#5) $-x+1, -y+2, z-1/2$; (#6) $-x, -y+2, z-1/2$; (#7) $-y+1, x-y+2, z$. Compound **4**: (#1) $-x+y, -x, z$; (#2) $x, y, z-1$; (#3) $y, -x+y, z+1/2$; (#4) $-x+y, -x+1, z-1$; (#5) $-x+1, -y+1, z-1/2$; (#6) $y, -x+y, z-1/2$.

we demonstrate a new strategy to synthesize metal chalcogenides using metal oxides in the air through the employment of a boron agent. The boron agent in the reactive system acts as a reducing agent because of its strong oxygen affinity, which can not only extract oxygen from metal oxides but also prevent the air, water, and silica tubes' disadvantageous influences on the syntheses. It is worth noting that the other advantage of this strategy is using low-cost rare-earth oxides instead of rare-earth elements or rare-earth sulfides, which are commonly used to synthesize multinary rare-earth sulfides.

Compounds **1**−**4** are isostructural to the $BLn_6M_2Q_{14}$ and $ALn_3MQ_7$ family compounds,[12] and each of them contains three types of building units: $AS_6$ (A = Al or Zn) octahedra, $MS_4$ (M = Al or Si) tetrahedra, and $LnS_8$ bicapped trigonal prisms (btp's; Figure 1). The Ln−S and Si−S bond lengths range widely from 2.716(3) to 3.530(1) Å and from 2.087(3) to 2.195(2) Å, respectively, in agreement with those found in this family compounds.[12] The crystal structures of **1**−**4** can be described as a 3-D Ln−S open framework, of which the 1-D channels along the *c* direction and tetrahedral holes are occupied by $AS_6$ (A = Zn, Al) chains and isolated $MS_4$ tetrahedra, respectively (Figure 2). Six $LnS_8$ btp's connect to each other by sharing faces to accommodate octahedral interspaces for $Zn^{2+}$ or $Al^{3+}$ cations, and three $LnS_8$ btp's create tetrahedral holes for M atoms by sharing corners. Until now, the B or A sites in $BLn_6M_2Q_{14}$ or $ALn_3MQ_7$ family compounds have been commonly occupied by monovalent alkali or coinage metal cations $Na^+$, $Ag^+$, and $Cu^+$, or divalent main-group metal cations $Mg^{2+}$, except for only two compounds ($Al_{0.44}La_3Si_{0.93}S_7$ and $In_{0.67}La_6Si_2S_{14}$) containing trivalent cations and four compounds ($MnLa_6Si_2S_{14}$, $NiLa_6Si_2S_{14}$, $CoLa_6Si_2S_{14}$, and $CdPr_6Ge_2S_{14}$) containing transition metal divalent cations.[12] The remarkable structural feature of **1** is that the octahedrally coordinated $Zn^{2+}$ cation is first introduced to B sites. Generally, the $Zn^{2+}$ cation is tetrahedrally coordinated by four S atoms and rarely adopts an octahedral coordination mode. As far as we know, only one inorganic compound ($ZnPS_3$)[21] in the ICSD and four metal-organic compounds in the CCDC[22] have $ZnS_6$ units like those in **1**. As the radius ratio of $Zn^{2+}$ (74 pm) to $S^{2-}$ (184 pm) is 0.402 and the $Zn^{2+}$ is of $d^{10}$ electron

(21) (a) Prouzet, E.; Ouvrard, G.; Brec, R. *Mater. Res. Bull.* **1986**, *21*, 195. (b) Boucher, F.; Evain, M.; Brec, R. *J. Alloys Compd.* **1994**, *215*, 63.

(22) (a) Helm, M. L.; Combs, C. M.; VanDereer, D. G.; Grant, G. J. *Inorg. Chim. Acta* **2002**, *338*, 182. (b) Sakane, G.; Kawasaki, H.; Oomori, T.; Yamasaki, M.; Adachi, H.; Shibahara, T. *J. Cluster Sci.* **2002**, *13*, 75. (c) Kuppers, H. J.; Wieghardt, K.; Nuber, B.; Weiss, J. *Z. Anorg. Allg. Chem.* **1989**, *577*, 155. (d) Setzer, W. N.; Guo, Q.; Grant, G. J.; Hubbard, J. L.; Glass, R. S.; VanDerveer, D. G. *Heteroat. Chem.* **1990**, *1*, 317.

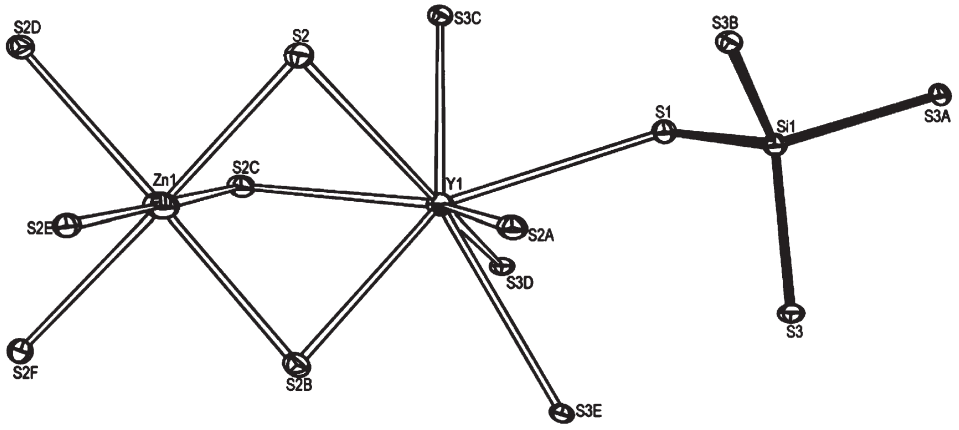


**Figure 1.** Coordination geometry of **1** with 50% thermal ellipsoids.

configuration, the $Zn^{2+}$ cation coordinated by four $S^{2-}$ ions can be well understood.[23] That is why there are so few compounds containing the $ZnS_6$ unit. In the $BLn_6M_2Q_{14}$ and $ALn_3MQ_7$ family compounds, their crystal structures are mainly dominated by the Ln−Q polyhedra due to the long radius of Ln cations, which construct octahedral cavities to accommodate different sized cations on B/A sites. Similar to $NiLa_6Si_2S_{14}$ and $CoLa_6Si_2S_{14}$, where the radii of $Ni^{2+}$ (72 pm) and $Co^{2+}$ (74 pm) cations are close to the radius of the $Zn^{2+}$ cation, although the octahedral cavity constructed by Ln−S polyhedra is a little large for these transition-metal cations, the $BS_6$ octahedra are face-shared to form a 1-D chain, which may benefit the stabilization of the crystal structure. The Zn−S bond distances in **1** fall in the range 2.537(2)−2.617(2) Å, which is comparable to the 2.562−2.575 Å in $ZnPS_3$.[21]

Unlike $Al_{0.44}La_3Si_{0.93}S_7$,[12c] in which the atoms on M sites are incompletely occupied by a Si atom, compounds **2** and **3** are the ones with Si/Al disorder on the M sites, and compound **4** is the first one with an occupancy of an $Al^{3+}$ cation on A sites that is well refined to one-third. The Al−S bond lengths on the A site in **2**−**4** are 2.504(4)−2.585(6) Å, which is comparable to the 2.582−2.590 Å in $Al_{0.44}La_3Si_{0.93}S_7$.

In order to satisfy the charge balance, the site occupancies of the Zn atom in **1** and Al atom in **4** were refined to 0.5 and 1/3, respectively, while the Al atoms on the A site in **2** and **3** are more than 0.33 in view of the Si/Al disorder on the M sites. The formulas of **2** and **3** are similar, but they are actually different compounds on the basis of the following three aspects: (1) Their unit cell parameters significantly differ from each other, which should arise from the different atomic occupancy of $Al^{3+}$ on the A site and the Si/Al disorder on the M site. (2) When the Al occupancies on the A site in **2** and **3** were refined to 0.50 and 0.38, respectively, their ADP parameters were normal and acceptable. (3) Their NLO properties are obviously different.

Usually, quaternary rare-earth thiosilicates have the following characteristics: (1) They have extensive transmission windows in mid- and far-IR. (2) The IVA element is usually tetrahedrally coordinated and often departs from ideal tetrahedral coordination. (3) Rare-earth elements Ln have high coordination numbers and generally displace from the center of their polyhedra. (4) Two kinds of metal centers usually have different sizes, coordination preferences, and packing characteristics. All of these factors make the probability of acentric arrangements largely increase. Compounds **1**−**4** crystallize in the chiral space group $P6_3$, which belongs to one of the 10 polar crystal classes (1, 2, 3, 4, 6, *m*, *mm*2, 3*m*, 4*mm*, and 6*mm*),[1] so they have potential applications in the region of NLO, piezoelectricity, pyroelectric, and ferroelectricity. In the study of NLO properties, they were first irradiated by 1064 nm laser light, but no green lights were observed due to their absorption in the visible-light region (Figure S2, Supporting Information). However, when they were irradiated by 2.1 $\mu$m laser light, the SHG intensities of **1**−**3** with a particle size of ∼20 um are about 2, 2, and 1 times that of graded KTP, respectively. No obvious SHG signal and about 0.3 times that of graded KTP were discovered for compound **4** with particle sizes of ∼20 um and ∼150 um, respectively. To date, only $CuLa_3GeSe_7$ in the $BLn_6M_2Q_{14}$ and $ALn_3MQ_7$ family compounds was reported to exhibit a weak SHG signal (about 30% that of quartz; the SHG response of KTP is more than 400 times that of quartz).[24] These results maybe provide a new strategy for the design of a stronger SHG effect by employing more $Al^{3+}$ ions that locate in the polar axis direction. Generally, laser damage thresholds of NLO materials are relative to their band gaps, which increase with an increase in band gap. The band gaps of **1**−**4** are in the range 2.0−2.4 eV (Figure S2, Supporting Information), which is comparable with those of the well-known IR NLO crystals $AgGaS_2$ (2.73 eV) and $ZnGeP_2$ (2.0 eV),[11] implying that the present compounds have suitable laser damage thresholds for NLO applications. Furthermore, the present compounds are transparent in the mid-infrared range (2.5−14.3 $\mu$m, Figure S3, Supporting Information), which is comparable with those of $AgGaS_2$ (0.48−11.4 $\mu$m) and $ZnGeP_2$ (0.74−12 $\mu$m). Therefore, the modified $BLn_6M_2Q_{14}$ and $ALn_3MQ_7$ family compounds may be good candidates for mid- and far-IR NLO materials.

In 1990, Abrahams predicted systematically new ferroelectric inorganic materials in space group $P6_3$.[13] He thought that the $BLn_6M_2Q_{14}$ and $ALn_3MQ_7$ family compounds were more likely to be described as asymmetric double-well potential ferroelectrics, so the investigation of the ferroelectric properties of this family is hence of interest. However, so far, ferroelectric behaviors of this family of compounds have not

(23) Pauling, L. *The Nature of the Chemical Bond*; Cornell University Press: Ithaca, NY, 1960.

(24) Poduska, K. M.; DiSalvo, F. J.; Min, K.; Halasyamani, P. S. *J. Alloys Compd.* **2002**, *335*, L5.

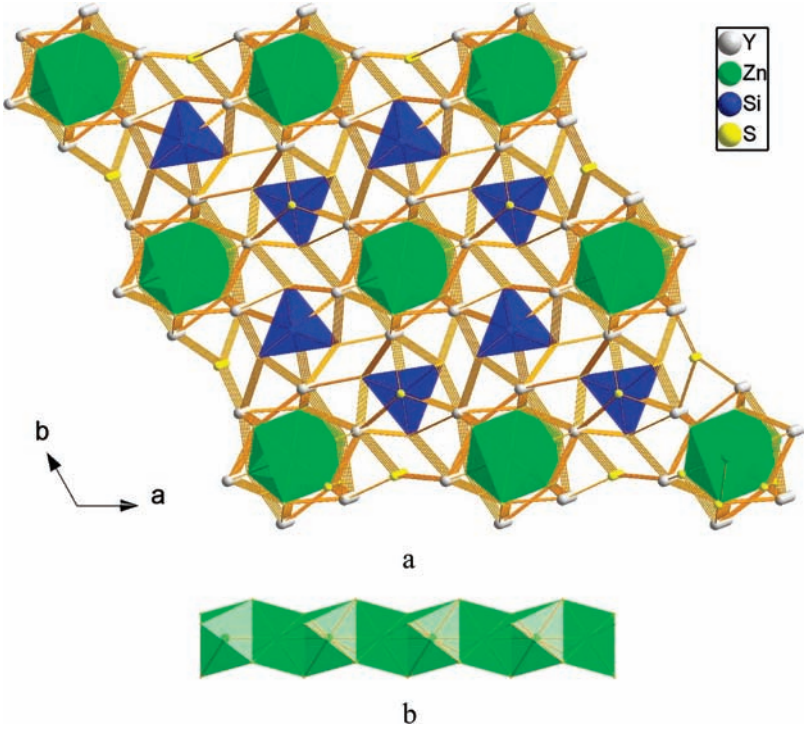


**Figure 2.** View of **1** along the *c* direction (a) and the 1-D face-sharing chain of $ZnS_6$ octahedra (b, green).

been reported. Unfortunately, large single crystals of **1**−**4** have failed to be obtained, so the ferroelectricity of **4** can only be studied by using a pellet of a powdery sample. As shown in Figure S4a (Supporting Information), ferroelectric hysteresis-like loops of variable voltages were observed, but macroscopic polarization reversal was not found, which implies that hysteresis-like loops may be derived from a lossy dielectric. Further ferroelectric hysteresis measurement using variable frequencies exhibits that the effect of a lossy dielectric also exists with increasing frequencies up to 3000 Hz (Figure S4b, Supporting Information), indicating that the remnant polarization of **4** mainly originates from the lossy dielectric, so compound **4** may reveal the absence of ferroelectric effects or extremely weak ferroelectricity.

Further interest in this study arises from the opportunity to observe the combination of NLO, ferroelectricity, and magnetism in $BLn_6M_2Q_{14}$ and $ALn_3MQ_7$ family compounds. The variable-temperature magnetic properties of **2**−**4** have been measured (Figure 3 and Figure S5, Supporting Information). As for **2**, the effective magnetic moment of three isolated $Dy^{3+}$ ions is determined to be 18.02 $\mu_B$ at room temperature, which is close to the theoretical value of 18.36 $\mu_B$ for three isolated free $Dy^{3+}$ ions. At 300 K, $\chi_M T$ is equal to 40.617 $cm^3$ K $mol^{-1}$. As the temperature is lowered, the $\chi_M T$ value decreases continuously to a value of 14.865 $cm^3$ K $mol^{-1}$ at 2 K. For **3**, the effective magnetic moment of three isolated $Dy^{3+}$ ions is determined to be 17.50 $\mu_B$ at room temperature, which is close to the theoretical value of 18.36 $\mu_B$ for three isolated free $Dy^{3+}$ ions. At 300 K, $\chi_M T$ is equal to 38.289 $cm^3$ K $mol^{-1}$. As the temperature is lowered, the $\chi_M T$ value decreases continuously to a value of 15.071 $cm^3$ K $mol^{-1}$ at 2 K. For **4**, the effective magnetic moment of three isolated $Sm^{3+}$ ions is determined to be 2.54 $\mu_B$ at room temperature, which is close to the theoretical value of 2.68 $\mu_B$ for three isolated free $Sm^{3+}$ ions. At 300 K, $\chi_M T$ is equal to 0.915 $cm^3$ K $mol^{-1}$. As the temperature is lowered, the $\chi_M T$ value decreases continuously to a value of 0.064 $cm^3$ K $mol^{-1}$ at 2 K. The magnetic behaviors of **2**−**4** indicate that antiferromagnetic-like interactions possibly exist between Ln(III) ions at low temperatures.

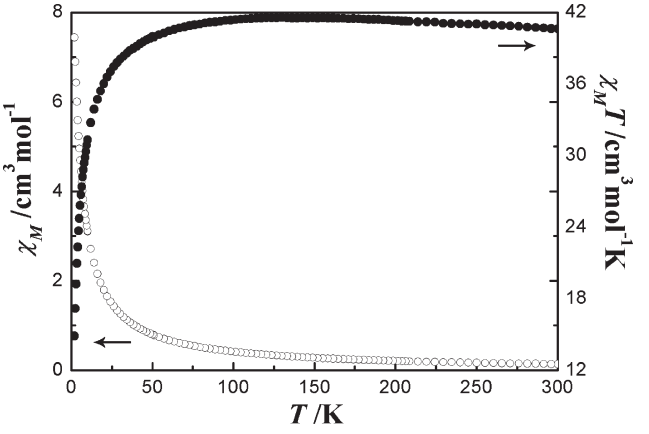


**Figure 3.** Plots of $\chi_M$ and $\chi_M T$ vs *T* for **2**.

The calculated band structure of **1** along high symmetry points of the first Brillouin zone is plotted in Figure S6 (Supporting Information). It is found that the tops of valence bands (VBs) have small dispersions. The lowest energy (2.13 eV) of conduction bands (CBs) is localized at the *K* point, and the highest energy (0.00 eV) of VBs is localized at the *G* point. Accordingly, the present compound shows semiconducting character with an indirect band gap of 2.13 eV, which is comparable with the experimental value (2.38 eV, Figure S2, Supporting Information). The bands can be assigned according to the total and partial DOS as plotted in Figure S7 (Supporting Information). The VBs between the energy level −5.0 eV and the Fermi level (0.0 eV) are mostly formed by the S−3p state mixing with small Y−5s, Y−4d,

and Si−3p states, while the CBs between 2.0 and 5.0 eV are almost a contribution from the Y−4d state hybridized with a small amount of S−3p, Si−3p, and Zn−3s states. Accordingly, it can be considered that the optical absorption of **1** is mainly ascribed to the charge transitions from S−3p to Y−4d states. Similarly, the optical absorptions of **2**−**4** can be mainly ascribed to the charge transitions from S−3p to Ln−4f states.

## Conclusion

We have prepared and characterized four new quaternary thiosilicates semiconductors, which exhibit novel NLO and antiferromagnetic-like properties. The optical studies show that compounds **1**−**3** exhibit the largest reported SHG effects at 2.1 um in the $BLn_6M_2Q_{14}$ and $ALn_3MQ_7$ family compounds, which enriches the study of IR NLO crystals.

**Acknowledgment.** We gratefully acknowledge the financial support of the NSF of China (20821061, 20701037), the NSF for Distinguished Young Scientist of China (20425104), the 973 program (2009CB939801), Key Project from the CAS (KJCX2.YW.M10), and the NSF of Fujian Province (2006J0013).

**Supporting Information Available:** Crystallographic file in CIF format and additional tables and figures. This material is available free of charge via the Internet at http://pubs.acs.org.